



ISSN: 0067-2904

Study of Some Plasma Characteristics in Dielectric Barrier Discharge (DBD) System

Murad M. Kadhim*, Qusay A. Abbas, Mohammed R. Abdulameer
Physics Dep., College of Science, University of Baghdad, Baghdad, Iraq

Received: 15/9/2021

Accepted: 29/11/2021

Published: 30/5/2022

Abstract

In this present paper, an experimental study of some plasma characteristics in dielectric barrier discharge (DBD) system using several variables, such as different frequencies and using two different electrodes metals (aluminium (Al) and copper (Cu)), is represented. The discharge plasma was produced by an AC power supply source of 6 and 7 kHz frequencies for the nitrogen gas spectrum and for two different electrodes metals (Al and Cu). Optical emission spectrometer was used to study plasma properties (such as electron temperature (T_e), electron number density (n_e), Debye length (λ_D), and plasma frequency (ω_{pe})). In addition, images were analysed for the plasma emission intensity at atmospheric air pressure.

Keywords: Dielectric Barrier Discharge (DBD), Optical Emission Spectroscopy (OES), Image J Software, Electron Temperature (T_e), Electron Number Density (n_e).

دراسة بعض خصائص البلازما في نظام تفريغ الحاجز العازل

مراد محمد كاظم*, قصي عدنان عباس, محمد رضا عبد الامي

قسم الفيزياء, كلية العلوم, جامعة بغداد, بغداد, العراق

الخلاصة

في هذا البحث نقدم دراسة تجريبية لبعض خصائص البلازما في نظام تفريغ الحاجز العازل (DBD) باستخدام عدة متغيرات مثل الترددات المختلفة واستخدام نوعين من الأقطاب الكهربائية مثل الألمنيوم والنحاس. تم إنتاج بلازما التفريغ بواسطة مصدر مجهز قدرة للتيار المتناوب بترددات 7 و 8 كيلو هرتز ولكلا المعدنين. تم استخدام مطياف الانبعاث البصري لدراسة خصائص البلازما (مثل درجة حرارة الإلكترون، الكثافة العددية للإلكترون، طول ديبي، وتردد البلازما). بالإضافة إلى تحليل الصور لشدة انبعاث البلازما عند ضغط الهواء الجوي.

1. Introduction

Dielectric barrier discharge (DBD) is the electrical discharge between two electrodes separated by an insulating dielectric barrier [1]. Volume or vertical discharge and surface discharge are the two types of DBD. Glass, quartz, ceramics, epoxy, and enamels are

*Email: murad.kadhim1204@sc.uobaghdad.edu.iq

common dielectric barrier materials. Other materials that can be used include plastic films, silicon rubber, Teflon plates, and others. DBD have been effectively employed in pollution control and to increase the wettability, printability, and adhesion of polymer surfaces. It has the potential to improve plasma chemistry and surface processing at atmospheric pressure. The main advantage of DBD over other approaches such as low-pressure discharges, fast-pulsed high-pressure discharges, or electron beam injection is that it is much easier to achieve non-thermal equilibrium plasma condition. DBD's flexibility in terms of geometrical arrangement, working medium, and operational parameters is another key advantage at atmospheric air pressure [2]. The dielectric works as a barrier, limiting current flow and preventing spark production, resulting in non-thermal discharges. This arrangement can be utilized to treat sensitive substrates like living textures without producing heat damage when used at atmospheric pressure. When a DBD is operated at high pressures (0.1 bar), the discharge breaks into multiple micro discharges that are evenly spaced and timed in the discharge gap or over the discharge region [3]. The volume discharge (VD) is the discharge that fills the gap between the electrodes, whereas the surface discharge (SD) is the discharge that occurs on the dielectric surface. The discharge that is created is responsible for the light intensity on the dielectric's surface [4].

In order to determine plasma parameters such as electron temperature (T_e), electron number density (n_e), Debye length (λ_D), and plasma frequency (ω_{pe}), optical emission spectroscopy (OES) has been used. The Boltzmann plot method is a straightforward and commonly used spectroscopic measurement technique, particularly for determining T_e [5]. Boltzmann distribution is satisfied in case of local thermodynamic equilibrium (LTE) [6,7].

$$\ln(\lambda_{mn} I_{mn} / hc g_m A_{mn}) = -E_m / kT_e + \ln(N/U) \quad (1)$$

Where: I_{mn} , λ_{mn} and A_{mn} are the intensity, wavelength and transition probability corresponding to transition from upper energy level (m) to lower energy level (n), g_m is statistical weight, h is the Planck's constant, $N = 1$ is the number density of emitting species, c is the speed of light, and $U = 1$ is a partition function.

The n_e was calculated using the Stark broadening effect, which requires a line that is free of self-absorption [8]:

$$n_e (\text{cm}^{-3}) = [\Delta\lambda / 2\omega_s] N_r \quad (2)$$

Where: $\Delta\lambda$ is the full width at half maximum (FWHM) of the line, and ω_s is the theoretical line full-width Stark broadening parameter, which is calculated at the same reference electron density $N_r = 10^{17} (\text{cm}^{-3})$.

Plasma frequency can be given as [9,10]:

$$\omega_{pe} = \sqrt{\frac{n_e e^2}{m_e \epsilon_0}} \quad (3)$$

Where ϵ_0 is the permittivity of free space, m_e is the mass of the electron and e is the charge of an electron.

Debye length can be calculated by the formula [8]:

$$\lambda_D = \sqrt{\frac{\epsilon_0 k_B T_e}{e^2 n_e}} \cong 69 \sqrt{\frac{T_e (\text{°K})}{n_e (\text{m}^{-3})}} \cong 743 \sqrt{\frac{T_e (\text{eV})}{n_e (\text{cm}^{-3})}} \quad (4)$$

Where: k_B is Boltzmann constant.

2. Experimental part

Figure 1 illustrated the AC dielectric barrier discharge (DBD) system that was used in this work. The electrodes are of cylindrical geometry and are made of aluminum or copper (with a thickness of 2 cm and a diameter of 3 cm for the cathode electrode and with a thickness of 3 cm and a diameter of 4 cm for the grounded anode). Both electrodes

are immersed in Teflon container to prevent electrical sparks in the edge of the electrodes. The gap distance between the two electrodes is 6 mm. The dielectric barrier (glass slide with a thickness of 3 mm) is inserted in the gap. The surface plasma was generated on the surface of dielectric barrier under atmospheric air pressure conditions. In this work, the discharge was produced when an AC constant voltage of 20 kV was applied between the two electrodes. Due to this external voltage, when the surface plasma discharge is formed, the voltage of the electrodes will drop. In addition, an ammeter and voltmeter are attached to the system to control the delivered electrical current and voltage, respectively. Images were taken for the glow within the plasma at different conditions (different applied voltage frequency and different metals of the electrodes : aluminum and copper) with a high-resolution mobile camera model (Samsung Galaxy Note 9) of (12Mpixel). The emission intensity of discharge regions in this system was analyzed using the image J software. Plasma emission spectrum was detected with an optical emission spectrometer (model Thorlabs, made in Germany) to determine plasma characteristics by diagnosing of the spatially integrated plasma light emissions for a wavelength range of 320-740nm. The spectrometer was placed at an angle of 45° from the plasma column. The results of the spectrum of this system were calibrated with NIST database software to calculate the plasma characteristics in the inter-electrodes gap.

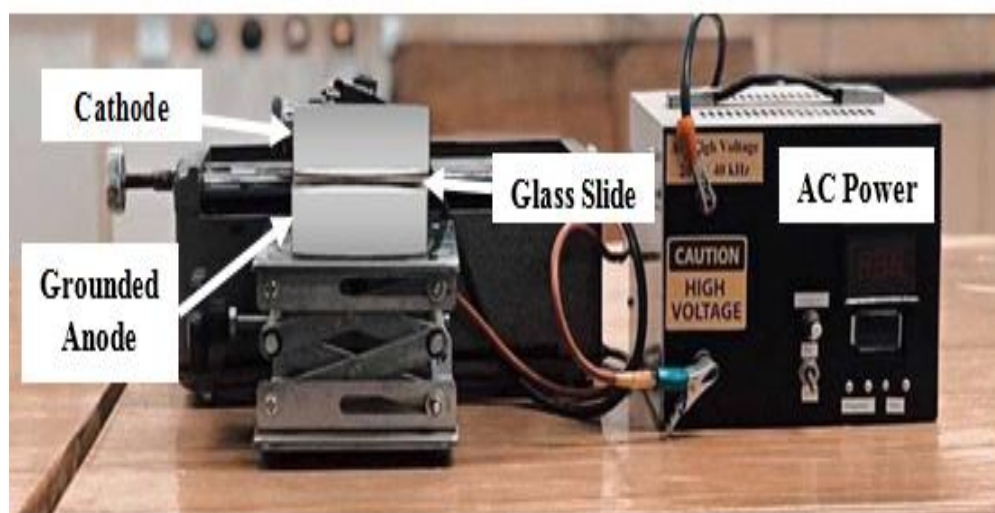


Figure 1-The DBD system.

3. Results and discussions

3.1 Glow Discharge Distribution

Figure 2 shows the influence of the applied voltage frequency on the surface discharge (SD) regions in the dielectric barrier discharge (DBD) system using different electrode metals (aluminum and copper), at atmospheric air pressure. The SD regions are responsible for almost all ionization and excitation processes that produce the plasma particles. In this figure, one can observe that as the frequency rises, the emission intensity rises as well. Because the increase of the applied voltage frequency leads to increase in the effect of the space charge as a result of plasma compressed and hence increasing the emission intensity. The emission intensity in the plasma spectrum for the copper electrode was less than that for the aluminum electrode with the same dimensions. Since the emission intensity depends on the work function of the electrode metal, the lower the work function of the metal, the lower the plasma emission intensity. This result agrees with Fitzpatrick [11].

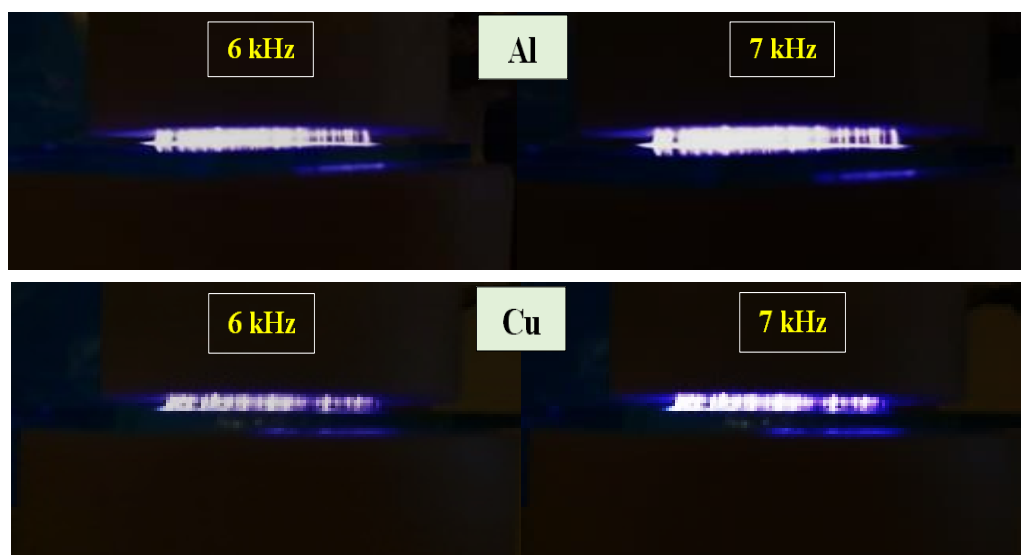


Figure 2- Image for glow distribution using DBD system at atmospheric air pressure.

3.2 I-V characte Figure 3 shows the influence of the applied voltage frequency on the I-V curves in the dielectric barrier discharge (DBD) system using different electrodes metals (aluminum and copper), at atmospheric air pressure. From the figure, it can be noticed that the I-V curve of the higher applied voltage frequency appeared at higher currents (with a higher rate in the aluminum electrodes compared with the copper electrodes), due to the increase of the electron density which causes more ionization collisions, hence, increase the I-V curves which essentially depend on electron density. This result agrees with that of Hassouba and Dawood[12].

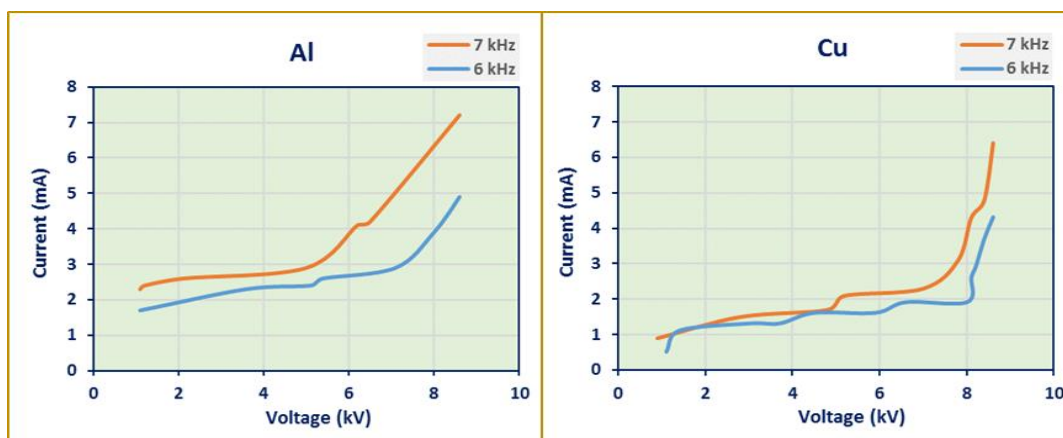


Figure 3- I-V curves for DBD system, using two electrodes of different metals (Al and Cu), at atmospheric air pressure.

3.3 Axial Profile of Emission Plasma Intensity

The emission intensity of surface discharge regions in this system was analyzed using the Image J software. Figure 4 represents the emission light intensity distribution in the gap between the two electrodes at atmospheric air pressure, for two frequencies (6 and 7 kHz) of the applied voltage using two electrodes of different metals (aluminum and copper). Many features can be obtained from this figure, the light intensity decreased in the plasma sheath near the electrodes surface. Also the emission intensity increases with increasing the applied voltage frequency (with a higher rate in the aluminum electrodes).

This increase may be caused by recombination or excitation of the nitrogen atoms which raised the light intensity in the central region. This result agrees with that of Awsi [13].

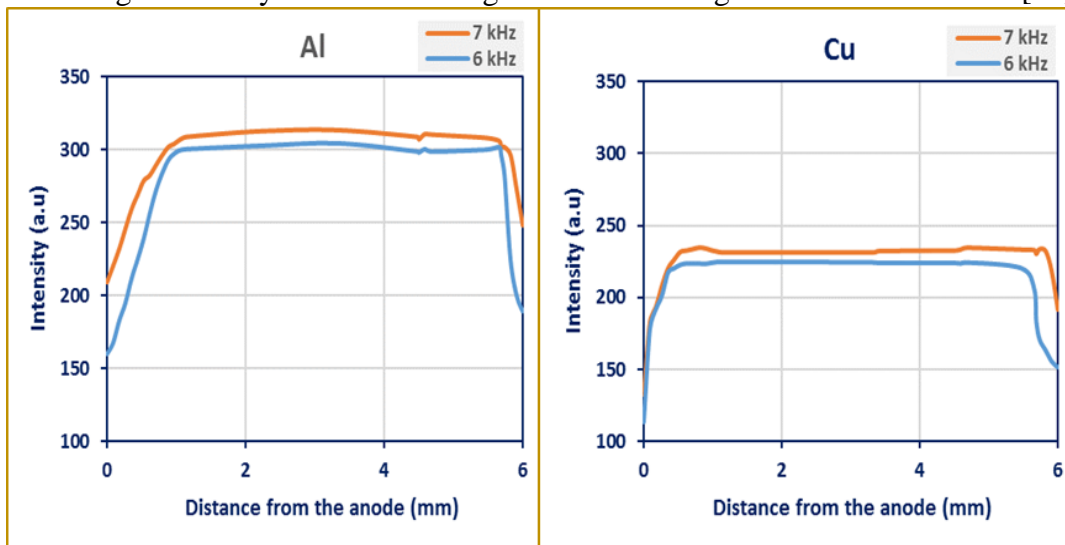


Figure 4-The variation of plasma emission intensity against distance from the anode for DBD system, at atmospheric air pressure.

3.4 Optical Emission Spectra

Plasma emission was detected by OES to determine the plasma characteristics by the diagnosis of the spatially integrated plasma light emissions for a wavelength range of 320-740nm. The emission spectrum of plasma produced in the gap between the entire surface of the electrodes at atmospheric air pressure, for two different frequencies (6 and 7 kHz) with two electrodes of different metals (aluminum and copper) is shown in Figure 5. From this figure, it can be noticed that there are many peaks of the nitrogen ionic (N II) lines that appear at the wavelengths 399.499, 435.222, 631.880, 701.473, and 715.675nm. The atomic emission lines of N I were also detected at the wavelengths 674.167 and 734.757nm, while peaks at 337.130, 357.690, 380.490 and 405.940nm corresponds to atomic emission lines of N₂ I. These peaks are of different intensities because of the varying probability of transition and the exciting levels of statistical weight. The intensity of all the peaks increased with an increase in frequency, with a higher rate for the aluminum electrodes compared to the copper electrodes, as a result of the difference of the work function of the two metals, where the work function effects the kinetic energy of the electrons which leads to more ionization collisions and thus an increase in the plasma emission intensity, due to an increase in the potential difference between the electrodes, which allows electrons to have enough excitation energy. This result agrees with that of Petitpas et al.[14].

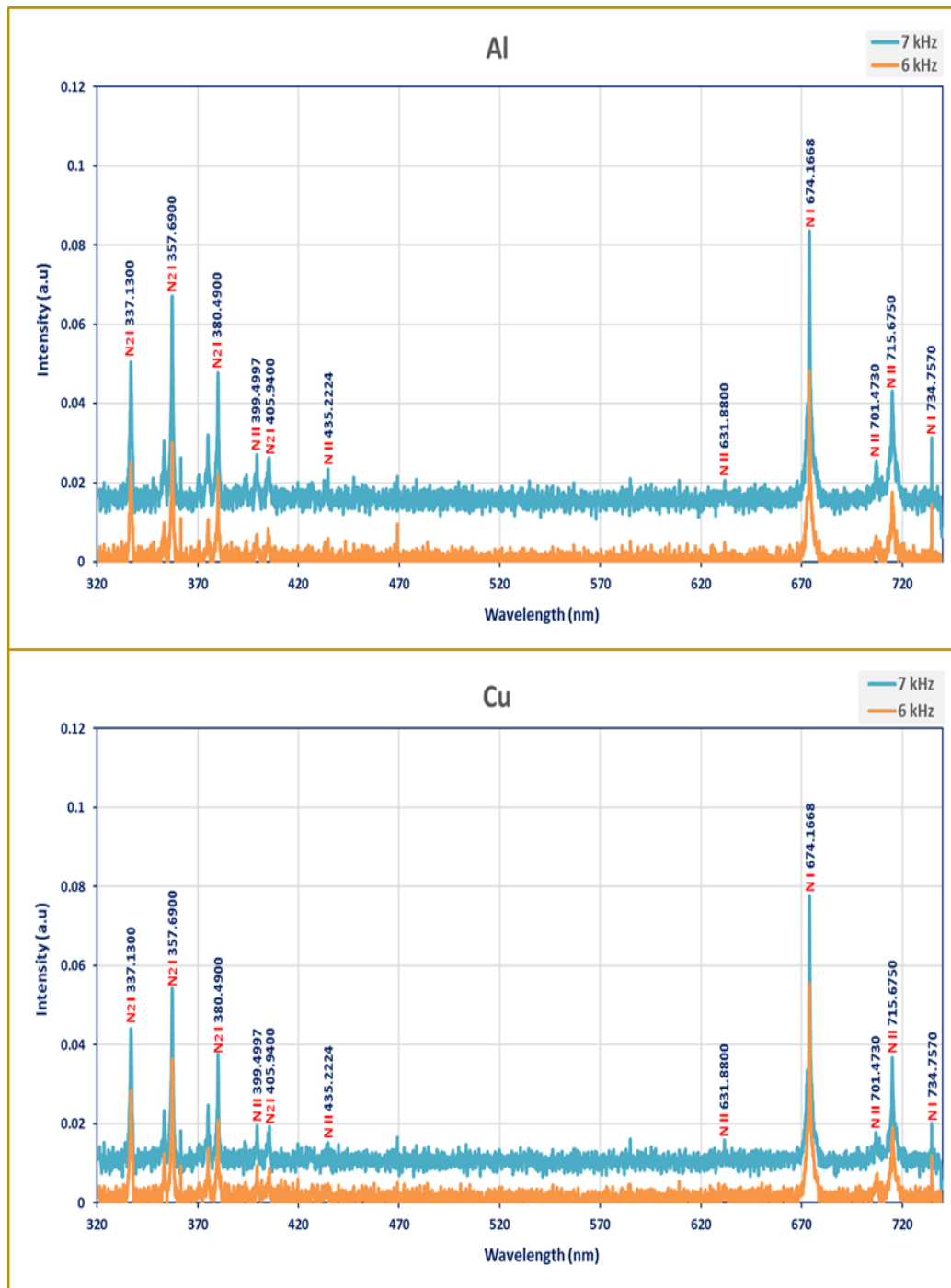


Figure 5-The optical emission spectra of DBD system, for two frequencies of the applied voltage using two electrodes of different metals (Al and Cu), at atmospheric air pressure.

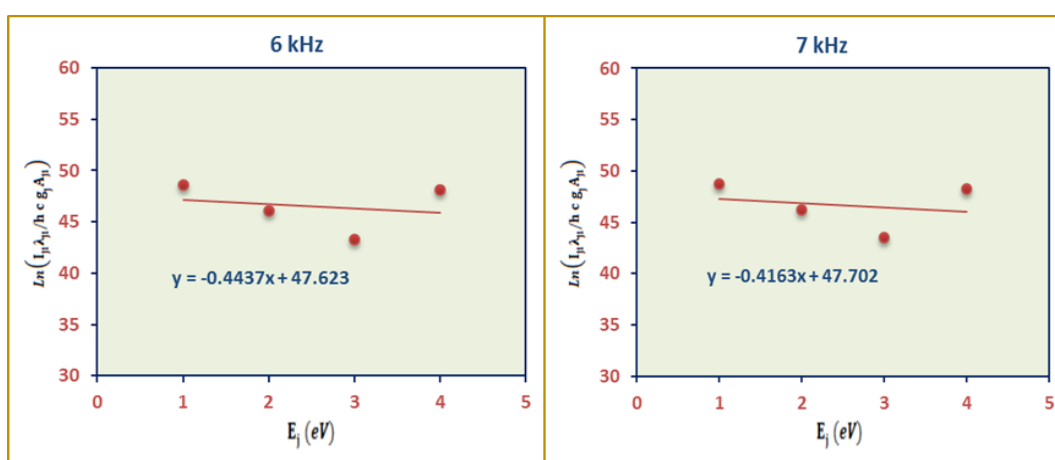
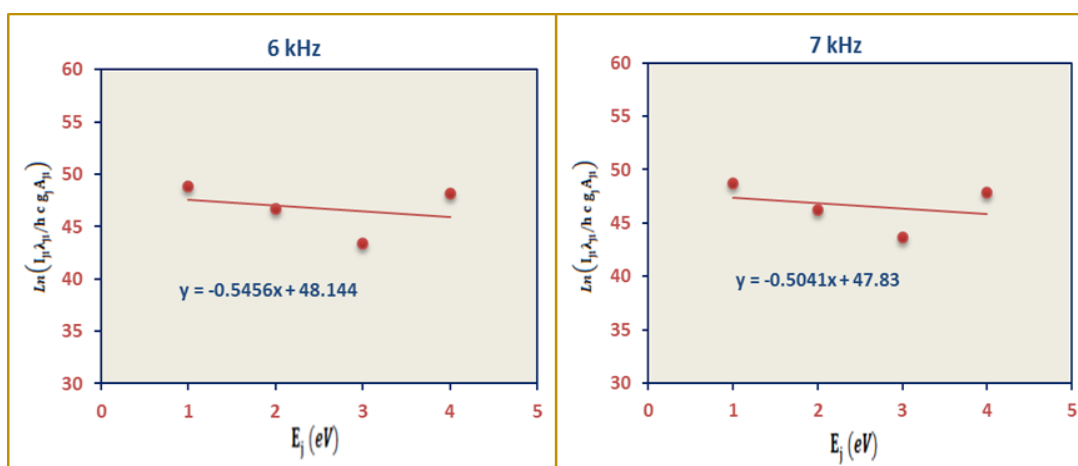
3.5 plasma characteristics

The value of T_e was calculated according to the Boltzmann plot method (Equation (1)) with the data listed in Table 1. By plotting $\ln(\lambda_{mn}I_{mn}/hc g_m A_{mn})$ versus upper energy level (E_j), the values of T_e is equal to the reciprocal of the slope for the best line fitting [15]. This necessitates peaks from the same ionic species with data from NIST.

Table 1- N II standard lines used to calculate electron temperature and their characteristics [16].

$\lambda(\text{nm})$	$A_{mn} \times g_m$	$E_i(\text{eV})$	$E_j(\text{eV})$
361.586	13×10^5	20.939965	24.367883
546.258	333×10^5	21.152682	23.421752
596.091	38.7×10^5	21.159916	23.239296
630.925	0.855×10^5	21.159916	23.124489

Figures 6 and 7 show the Boltzmann plots using the selected ionic nitrogen lines (N II) for the dielectric barrier discharge (DBD) system, in the cases under study at two different frequencies (6 and 7 kHz) and for the different metals of the electrodes.

**Figure 6-**Boltzmann plot for N II peaks using the DBD system at two different frequencies, with aluminum electrodes.**Figure 7-**Boltzmann plot for N II peaks using the DBD system at two different frequencies, with copper electrodes.

n_e can be calculated by Equation (2), which is called the Stark broadening effect. Based on the typical values of broadening for this line, FWHM values were used to compute n_e using the Stark effect ($N_r = 10^{17} \text{ cm}^{-3}$) [17].

Table 2 shows the calculated values of n_e , T_e , ω_{pe} , and λ_D for DBD plasma, using different electrodes metals (Al and Cu), at atmospheric pressure. The increase of the applied voltage frequency (f) led to the increase of the free electrons (which means the

increase of T_e), increase of the electron number density (n_e) (as a result of increase of the probability of the ionization collisions) and decrease of Debye length (from Equation (4)). These behaviors mean that the increase of electron number density with increasing the applied voltage frequency gave lower Debye length, while the Debye length decreased with the increase in the electron temperature. In general, the values of T_e , n_e , ω_{pe} , and λ_D with Al electrodes were higher than those for the Cu electrodes due to the increase in work function of the metal [18].

Table 2-Plasma parameters for the dielectric barrier discharge (DBD) system using different electrodes metals (aluminum and copper), at atmospheric air pressure.

Type of Electrodes	f (kHz)	T_e (eV)	$n_e \times 10^{17}$ (cm^{-3})	$\omega_{pe} \times 10^{11}$ (rad/sec)	$\lambda_D \times 10^{-6}$ (cm)
Al	6	2.254	8.026	506.339	1.245
	7	2.402	8.909	533.478	1.220
Cu	6	1.833	7.047	474.476	1.198
	7	1.984	7.633	493.809	1.197

Conclusion

In the present study, the effects of applied voltage frequency and type of electrode material on the properties of plasma were investigated. The present results illustrate that the values of the discharge current in the aluminum electrodes are larger than those in the copper electrodes. Thus, the slopes of the I-V curves in the aluminum electrodes are larger. In the DBD system, it was observed that increase of applied voltage frequency resulted in the increase of the plasma emission intensity (with a higher rate in the aluminum electrodes) and plasma characteristics like T_e , n_e , and ω_{pe} but caused a decrease in λ_D . The values of T_e , n_e , ω_{pe} , and λ_D for the Al electrodes were higher than those of the Cu electrodes.

References

- [1] G.J. Pietsch and V.I. Gibalov, "Dielectric barrier discharges and ozone synthesis", *Pure and Applied Chemistry*, vol.70, no. 6, pp. 1169-1174, 1998.
- [2] D. P. Subedi, U. M. Joshi, and C. San Wong, "Dielectric barrier discharge (DBD) plasmas and their applications," in *Plasma Science and Technology for Emerging Economies*, pp. 693-737, Springer 2017.
- [3] Y.Wu, Y. Li, M. Jia, H. Song, Z. Guo, X. Zhu, and Y. Pu, "Influence of operating pressure on surface dielectric barrier discharge plasma aerodynamic actuation characteristics," *Applied Physics Letters*, vol. 93, no. 3, pp. 031503, 2008.
- [4] U. Kogelschatz, "Dielectric-barrier discharges: their history, discharge physics, and industrial applications," *Plasma Chem. plasma Process*, vol. 23, no. 1, pp. 1-46, 2003.
- [5] A. Arshad, S. Bashir, and A. Hayat, M.Akram, A.Khalid, N. Yaseen and Q. S.Ahmad "Effect of magnetic field on laser-induced breakdown spectroscopy of graphite plasma," *Appl. Phys. B*, vol. 122, no. 63, pp. 1-10, 2016.
- [6] H. Conrads and M. Schmidt, "Plasma generation and plasma sources," *Plasma Sources Sci. Tech.*, vol. 9, no. 4, pp. 441-454, 2000.
- [7] T. A. Hameed, and S. J. Kadhim, "Plasma diagnostic of gliding arc discharge at atmospheric pressure," *Iraqi Journal of Science*, vol. 60, no. 12, pp. 2649-2655, 2019.
- [8] R.N. Fianklin, "Plasma Phenomena in Gas Discharges," *Oxford University Press, Oxford*, 1976.
- [9] F. Llewellyn Jones, "Ionization and Break down in Gases," *New York: John Wiley & Sons Inc.*, 1957.

- [10] Y. K. Jabur, M. G. Hammed, and M. K. Khalaf, "DC Glow Discharge Plasma Characteristics in Ar/O₂ Gas Mixture," *Iraqi Journal of Science*, vol. 62, no. 2, pp. 475-482, 2021.
- [11] R. Fitzpatrick, "Introduction to plasma physics," Univ. Texas Austin, 2006.
- [12] M. A. Hassouba, and N. Dawood, "Study the effect of the magnetic field on the electrical characteristics of the glow discharge," *Advances in Applied Science Research*, vol. 2, no. 4, pp. 123-131, 2011.
- [13] S. K. Awsi, "Effect of nitrogen gas pressure and hollow cathode geometry on the luminous intensity emitted from glow discharge plasma," *Am. J. Mod. Phys.*, vol. 2, no. 6, pp. 276–281, 2013.
- [14] G. Petitpas, J.-D. Rollier, A. Darmon, J. Gonzalez-Aguilar, R. Metkemeijer, and L. Fulcheri, "A comparative study of non-thermal plasma assisted reforming technologies," *Int. J. Hydrogen Energy*, vol. 32, no. 14, pp. 2848–2867, 2007.
- [15] H. Park, S. J. You, and W. Choe, "Correlation between excitation temperature and electron temperature with two groups of electron energy distributions," *Phys. Plasmas*, vol. 17, no. 10, pp. 1–4, 2010.
- [16] NIST Atomic Spectra Database." [Online]. Available: [https:// www.nist.gov/pml/atomic-spectra-database](https://www.nist.gov/pml/atomic-spectra-database), 2020.
- [17] N. Konjevic, A. Lesage, J. Fuhr, and W. Wiese, "Experimental Stark widths and shifts for spectral lines of neutral and ionized atoms," *J. Phys. Chem. Ref. Data*, vol. 31, no. 3, pp. 1307–1385, 1990.
- [18] U. Kogelschatz, "Dielectric-barrier discharges: their history, discharge physics, and industrial applications," *Plasma Chem. plasma Process.*, vol. 23, no. 1, pp. 1–46, 2003.